NASA CR- 166,602

NASA-CR-166602
19840026357

NASA CONTRACTOR REPORT 166602

(NASA-CR-166602) WAKE PROFILE MEASUREMENTS OF FIXED AND OSCILLATING FLAPS (Compass Systems, Inc., San Diego, Calif.) 38 p HC A03/MF A01 CSCL 01A

N84-34428

Unclas
G3/02 22946

Wake Profile Measurements of Fixed and Oscillating Flaps.

F. K. Owen

CONTRACT NAS2-11080
April 1984

NASA CONTRACTOR REPORT 166602

Wake Profile Measurements of Fixed and Oscillating Flaps.

F. K. Owen,
Complere Inc.,
P.O. Box 1697,
Palo Alto, CA 94302.

Prepared for
Ames Research Center,
under Contract NAS2-11080

National Aeronautics and
Space Administration

Ames Research Center
Moffett Field California 94035

ABSTRACT

In December 1982 a series of laser velocimeter measurements of the near wake of a 2-D NACA 64A010 airfoil model were obtained in the Ames 11 Foot Wind Tunnel. This work was undertaken in support of an extensive investigation to evaluate the periodic pressure distributions and loads on the wing which had an oscillating, trailing edge flap. The purpose of this report is to evaluate and document the laser velocimeter measurements and compare the results with hot wire measurements obtained at several locations in the wake.

Nomenclature

u, v	Streamwise and vertical velocities (m/s)
x, y	Streamwise and vertical distances from airfoil trailing edge (cm)
α	Airfoil angle of attack (deg)
δ	Flap displacement (deg)
'	Denotes RMS velocity (m/s)
e	Denotes edge value

INTRODUCTION

Tail flutter in aeroplanes and the howling of propellers in steamships provide unpleasant examples of self-excited oscillations. However, conditions in which the external source of energy is the freestream can pose more than a nuisance. In fact the interaction between elastic, inertial and dissipative forces with imposed unsteady aerodynamic forces can have disasterous results. Consequently "flutter free" design demands are often governing factors.

Unfortunately the unsteady aerodynamics of both fixed and rotary wing aircraft is not yet sufficiently understood to provide safe margins for flutter or buffet without recourse to experiment and computation. Experience has shown that flutter problems are most severe in transonic flows. It is in this range, between Mach numbers of 0.8 and 1.5, which generally include regions of supersonic as well as subsonic flow, a combination of two profoundly different flow, regimes. Here, instruments for flowfield measurement may have significantly disturbing effects on the local flow parameters. Thus accurate documentation of cause and effect is difficult.

Of particular concern in the use of total head and hot-wire probes at transonic speeds is the ever present problem of flow interference. Wake flows are extremely sensitive to local geometry with streamline curavature and associated mean static pressure gradients rendering pitot tube mean flow measurements subject to error. Problems associated with turbulent structure measurements are even more acute since, at transonic

speeds, separation of the measured mode variables namely mass flux and total temperatures into velocity fluctuation and shear stress is a complex task. As a result, hot-wire turbulence data taken even in zero pressure gradient, adiabatic or isothermal attached boundary layers show considerable scatter (Ref 1).

Although more costly, laborious and tedious to operate,the laser velocimeter probably represents the instrument of last resort for the measurement of many practical flow fields. Once in operation, nonintrusive, unambiguous mean and turbulent velocities can be measured.

In 1982 an experiment in which steady and unsteady surface pressure distributions were measured on an airfoil with an oscillating flap was conducted in the Ames 11-foot wind tunnel (Ref. 2). This test was designed to provide an extensive data base for active controls and data to compare with computations (Ref. 3). Hot wire and Kulite measurements were also made behind the oscillating flap to determine steady and unsteady wake profiles (Ref. 4). However, since hot wire measurements had not been previously attempted in such a severe environment, it was decided to obtain redundant flow field data with laser velocimetry. This not only insured against failure of either method but also helped to determine the extent of reliable hot-wire application for transonic flutter studies.

As laser velocimeter measurements had not been previously attempted in this facility an evaluation was undertaken by Complere Inc, prior to the oscillating flap experiment. This task required the design and

fabrication and assembly of an optical configuration that was compatible with the physical layout of the 11-foot tunnel. For this work, which was carried out as an adjunct to a scheduled test, color separation and a parallel beam matrix was achieved on an optical bench outside the tunnel. Transmitting and receiving optics were mounted inside the plenum where both forward and back-scattered light was collected and photo multiplier outputs preamplified before processing by the self-contained laser velocimeter electronics in the control room. Measurements were obtained in the freestream along the tunnel center line.

Although tunnel test time was severely limited (<30 minutes) the test confirmed LDV feasibility since, in the forward scatter mode, data rates of several hundred per second could be achieved even with low laser power (~ 0.5W). However, it was evident that tunnel seeding would be required for the oscillating flap test to keep test time reasonably short and within acceptable costs.

EXPERIMENTAL DETAILS

Test Model

The experiment was conducted on a 2-D NACA 64A010 wing model with an oscillating, trailing edge flap hinged at 75 percent chord.

The model which had a 0.5m chord and 1.37m span was mounted in rotatable plates imbedded in vertical splitter plates which spanned the test section (fig. 1a). Test conditions were varied from 0.5 to 0.85 Mach number at stagnation pressures from 1/2 to two atmospheres. The incidence of the airfoil and flap could be varied over a wide range and the flap could be oscillated up to a frequency of 60 Hz with an amplitude of $\pm$ 6 degrees.

Laser Velocimeter

Velocity measurements were made in the near wake with the laser velocimeter shown schematically in Fig 1b. This system was designed and assembled by Complere Inc. and built by NASA Ames. This fringe-mode velocimeter is a dual-color system utilizing the 4880 and 5145 Angstrom lines of an argon-ion laser. One spectral line is used to measure the streamwise velocity component, the other to measure the vertical velocity component. Bragg-cell frequency shifting, which is necessary for probing highly turbulent and separated flow regions, is incorporated in both spectral lines. The frequency offsets also facilitate the direct measurement of the vertical velocity component (i.e., $\pm$ 45° beam orientations to resolve the vertical velocity are unnecessary).

As seen in Fig. 1b, the laser and most of the optical components are located outside the tunnel plenum chamber, where color separation, Bragg-cell frequency shifting, and the establishment of the four-beam matrix are accomplished. Only the transmitting optics, collecting lens, and photo detectors are mounted inside the plenum chamber. This precludes laser cavity pressure problems and helps ease alignment difficulties. Two traversing systems are shown inside the plenum chamber. The one on the opposite side of the test section from the laser holds the collecting lens and photo detectors for forward-scatter light collection. The traversing system on the laser side of the test section supports the transmitting lenses. Mirrors fixed to this traversing system permit two-dimensional scanning of the velocimeter's sensing volume; the optics outside the plenum chamber remain stationary. Both traversing systems are driven with computer-controlled stepper motors

The effective sensing volume is approximately elliptic, 200 um in diameter and 3 mm long, with the axis aligned in the cross-stream direction. Measurements were made in the near wake at 2.5 and 12.7 cm from the flap trailing edge at a Mach number of 0.8 and a stagnation pressure of one atmosphere, i.e., a chord Reynolds number of 6.5 million. Static data were obtained at three different airfoil and flap angle settings. Dynamic measurements were taken at a flap oscillation frequency of 30 Hz which corresponds to a reduced frequency of 0.35 based on the airfoil chord.

Seeding

Maximum optical system sensitivity is essential for meaningful measurements particularly in large wind tunnels. In these applications solid angle light collection is reduced so that there is always the possibility that only the velocities of larger particles, which may not follow the flow, will be observed. This could result in errors in the mean flow and turbulence measurements and difficulty in obtaining data in vortex cores. Previous measurements have stressed the value of forward scatter optical systems whenever possible, since data rates which are orders of magnitude higher than those in the back scatter mode can be achieved. Rather than relying entirely on natural wind-tunnel aerosols for the light scattering, it is advisable to introduce an artificial aerosol of known size distribution which can be generated with an ultrasonic nozzle mounted in the wind tunnel. The size distribution of such an aerosol with a count mean diameter of less than one micron is shown in Fig. 2. Such aerosols have been found adequate for turbulence studies of shock boundary-layer interactions and vortex flows at transonic

and supersonic speeds. To confirm this, axial and vertical velocity measurements have been previously obtained at variable threshhold settings on the processing electronics (Ref. 5). At high settings, only a few of the larger particles which passed through the center of the probe volume were considered, whereas at low threshhold settings velocities of the submicron particles dominated. Even in vortex cores, the mean flow angle varied less than 3° with threshhold setting changes which reduced the velocity data rate from 16,000/sec to 1,000 sec. These results were in substantial agreement with data obtained with natural seeding. So that, in general, seed material need only be introduced when high data rates necessary for conditional sampling or spectra measurements are required.

In the current experiment seeding was achieved with the installation of a Sonimist (model 500) nozzle which was mounted on the downstream side of the turning vanes ahead of the settling chamber in the center of the tunnel with the outlet pointing downstream. Although this produced a sufficient supply of scattering centers for the steady flow measurements it was barely adequate (maximum of 1000/sec) for the time dependent measurements. The seeder was controlled by an air pressure valve actuator located in the control room.

Data Acquisition

In addition to computer software, the data reduction system consists primarily of three elements: signal processors, an event synchronizer and a desk top computer. These elements are shown schematically in Fig. 3.

Each processor output contains the information required to calculate the instantaneous velocities u, v. From these determinations, the average velocities $\overline{u}$, $\overline{v}$, RMS turbulence levels u', v', and the cross correlations $\overline{u'v'}$, are all calculated. Plots of these parameters are displayed on line as profiles are measured and hard copy is available as required. All the raw and reduced data are stored on flexible discs for permanent storage and retrieval. Real time histograms, probability densities of all three velocity components are displayed during data acquisition.

A two-dimensional unsteady flow program for LDV data reduction is also available. Unfortunately, laser velocimeter data are usually difficult to conditionally sample since in most cases the data rates are insufficient to generate real-time information from which the sampling criteria can be determined. A technique close to conditional sampling can be used to generate ensemble averages at given phase angles in turbulent flows superimposed on periodic motions, such as those in reciprocating machinery or helicopter wakes, for example. In these cases, the sampling condition can be derived from a periodic timing signal.

A schematic of the two component measurement procedure used in the present test, is shown in Fig. 4 where the internal clock of the event synchronizer (multiplexer) is reset by an external pulse. In this case, readings from the multiplexer now contain information to calculate two instantaneous velocity components and time of arrival. From these determinations ensemble averages, throughout the unsteady period, can be generated. For each "data window," which can be

varied, $\overline{u}$, $\overline{v}$, u', v' and $\overline{u'v'}$ are calculated and displayed on line along with the histograms. At the conclusion of each profile, plots can be generated. Once again all the raw and reduced data are permanently stored on flexible discs.

In the present test, positioning and sinusidal oscillation of the flap was accomplished by servo controlled hydraulic acuators which drove the flap through vertical push rods in the splitter plates. The external reset pulse for the multiplexer clock was obtained from this flap drive mechanism.

RESULTS

Static Measurements

Laser velocimeter data obtained at fixed airfoil angles of attack of zero and four degrees with fixed flap angles of zero and minus four degrees are tabulated and plotted in Figs 5-9. Figs 5 and 6 show the symmetry of the axial velocity profiles in the near wake at zero angles of attack. In these cases there was excellent similarity between the laser velocimeter and pitot wake profiles. The axial and vertical velocity profiles show symmetric flow angularity consistent with wake closure and recovery downstream. Close inspection of the RMS axial velocity fluctuations, particularly at 12.7 cm, reveals double peaks, one on each side of the wake center line close to the regions of maximum mean velocity gradient. This implies that an eddy viscosity formulation could describe the shear layer behavior.

On the other hand when the airfoil and flap angles are increased (Figs. 8 and 9) RMS levels no longer scale with the local mean gradients,

and wake recovery increases at a rate which is approximately 50 percent faster. Calculated turbulent length scales estimated from the wake width and the ratio of the RMS levels wot wake velocity defect, increase by a factor of two. In this case it is clear that large scale turbulent mixing dominates and that these energetic motions lead to more rapid wake recovery.

Although there was similarity between the laser velocimeter and pitot profiles at zero angles of attack (Ref. 4), at 4 degrees there are marked differences (Fig 10). Although true axial velocity is difficult to determine from pitot profiles the probe indicates incipient separation, whereas the velocimeter profiles show only a thick retarded upper layer with significant entrainment and a thinner attached lower boundary layer. However, the measured surface pressure distributions were identical during both sets of measurements.

After wire calibration, direct comparisons can be made between the hot-wire (Ref. 4) and laser velocimeter measurements. These comparisons are shown in Figs 11 to 15 where the square symbols denote LDV data. At zero angles of attack (Figs 11 and 12) the axial velocity profiles compare quite well although the wire data suggest a wider wake close to the flap trailing edge. Agreement between the vertical velocity profiles is not as good. A zero shift in the hot wire data seems to be present especially in the downstream profile (Fig 12). On the other hand, there is good agreement between the vertical velocity profiles in Fig 13 whereas the hot-wire axial profile shows greater wake deficit with less displacement, i.e. below the actual location of the flap trailing

edge. Close to the flap at four degrees angle of attack (Fig 14) the agreement is poor, the hot-wire data show a severely retarded upper layer which is much thicker than the laser velocimeter profile. Agreement between the two vertical velocities is poor once again suggesting a zero offset in the hot wire data. Further downstream (Fig 15), the wake profiles disagree in both deficit and location and there is no correspondence between the two vertical velocity profiles. Computed flow angularity from the laser velocimeter data show downwash whereas the hot-wire data suggest upwash. Spanwise flow non-uniformities could explain these discrepancies.

Dynamic Measurements

For the cases of flap oscillation the LDV data rate was insufficient and too inconsistently distributed to obtain cycle to cycle information. Accordingly, the total number of velocity readings was divided among several flap angle windows and conditionally sampled over many cycles. If some windows were filled before others, they continued to accept readings, replacing the older data within their own windows. This ensured that only the most current data were reduced.

Ensemble-averaged measurements for the case of 30 Hz flap oscillation are shown in Figs. 16-18 for zero fixed airfoil angle of attack and a mean flap position of -4 degrees. This sequence shows that at -2 degrees flap angle the upper surface flow is once again retarded by the adverse pressure gradient, at -4 degrees the wake deficit and width are increased and at 6 degrees significant wake displacement can also be seen in addition to still greater wake effects. A comparison of the measured vertical

velocities shows increased wake deflection angles with increasing flap deflection.

Comparison of the static and dynamic results for a flap angle of -4 degrees (Figs. 7 and 17) shows that the dynamic profile has a wider wake and larger turbulent mixing length consistent with the time dependent shedding of large scale free vorticity, the result of periodic circulation variations. Admittedly though, the wider dynamic wake could also be due to the wider data measurement window and flow field jitter which leads to differences between the most likely and probability density function mean profiles and RMS levels. In general the most likely profiles are sharper with low RMS turbulence levels. PDF profiles tend to be smeared with higher RMS values. Comparisons of the laser and hot-wire velocity measurements, averaged over the same data windows are shown in Figs 19-21. In most of these cases agreement is only fair, the hot-wire showing greater wake deficits and widths but virtually no upward wake deflection as the flap angle increases. The vertical velocity profiles have similar shapes although their signs and magnitudes are often quite different.

CONCLUDING REMARKS

Conventional and ensemble-averaged laser velocimeter measurements have been accomplished for several test conditions in the 11-by-11 foot wind tunnel at NASA Ames Research Center. These measurements demonstrate the potential of the laser velocimeter for applications in other than closely controlled, small-sale laboratory situations. However, before extensive large-scale research programs are undertaken

in major wind tunnels, attention must be directed to remote optical alignment capability. This will enable longer run times and more efficient tunnel operation. For time dependent measurements, increased seeding density will probably be required.

Comparisons of the laser velocimeter and hot-wire measurements in the near wake show some inconsistencies between the two techniques which appear to be accentuated for the cases of flap oscillation. However, these results should still provide challenging test cases for computation.

References

1. Owen, F. K. "An Assessment of Flow-Field Simulation and Measurement," AIAA Invited Paper No. 83-1721, 1983.

2. Buell, D. A. and Malcolm, G. N. "Experimental Investigation of a 64A010 Airfoil with Oscillating Flap." Proposed NASA TM.

3. Horiuti, K., Chyu, W. J., and Buell, D. A. "Unsteady Flow Computations on an Airfoil with Oscillating Flap." Proposed NASA TM.

4. Bodapati, S. and Lee, C. S. "Unsteady Wake Profiles of an Oscillating Flap at Transonic Speeds." NASA CR (in preparation).

5. Owen, F. K. and Johnson, D. A. "Wake Vortex Measurements of Bodies at High Angles of Attack," AIAA Paper No. 78-23, 1978.

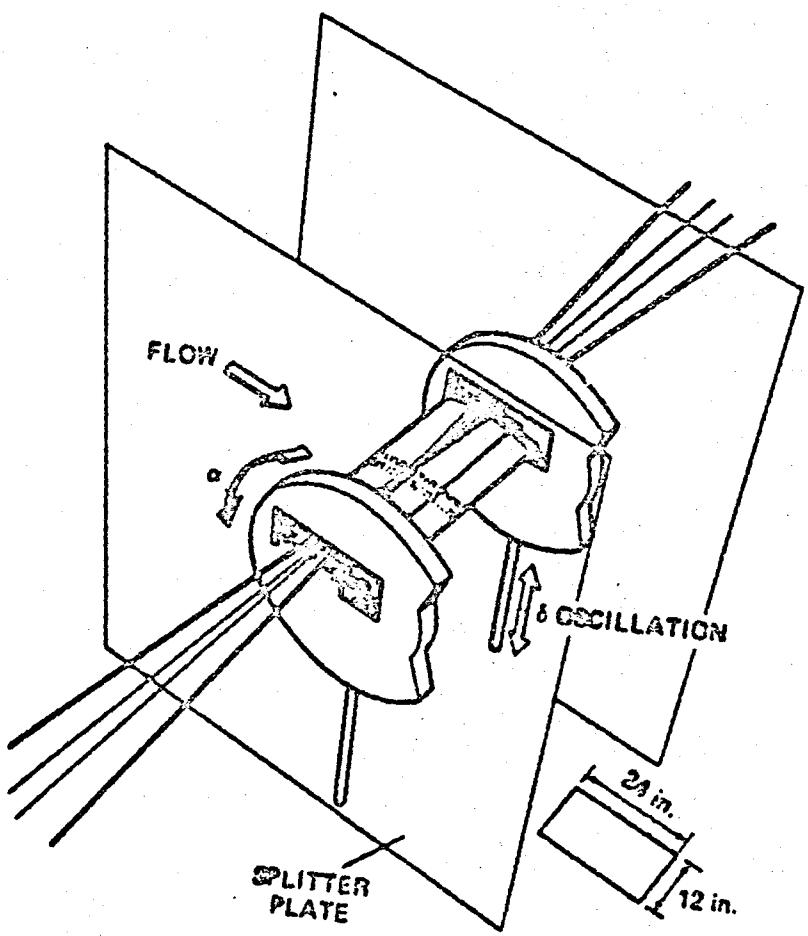

Fig. 1a Model Installation in Ames 11-foot Wind Tunnel

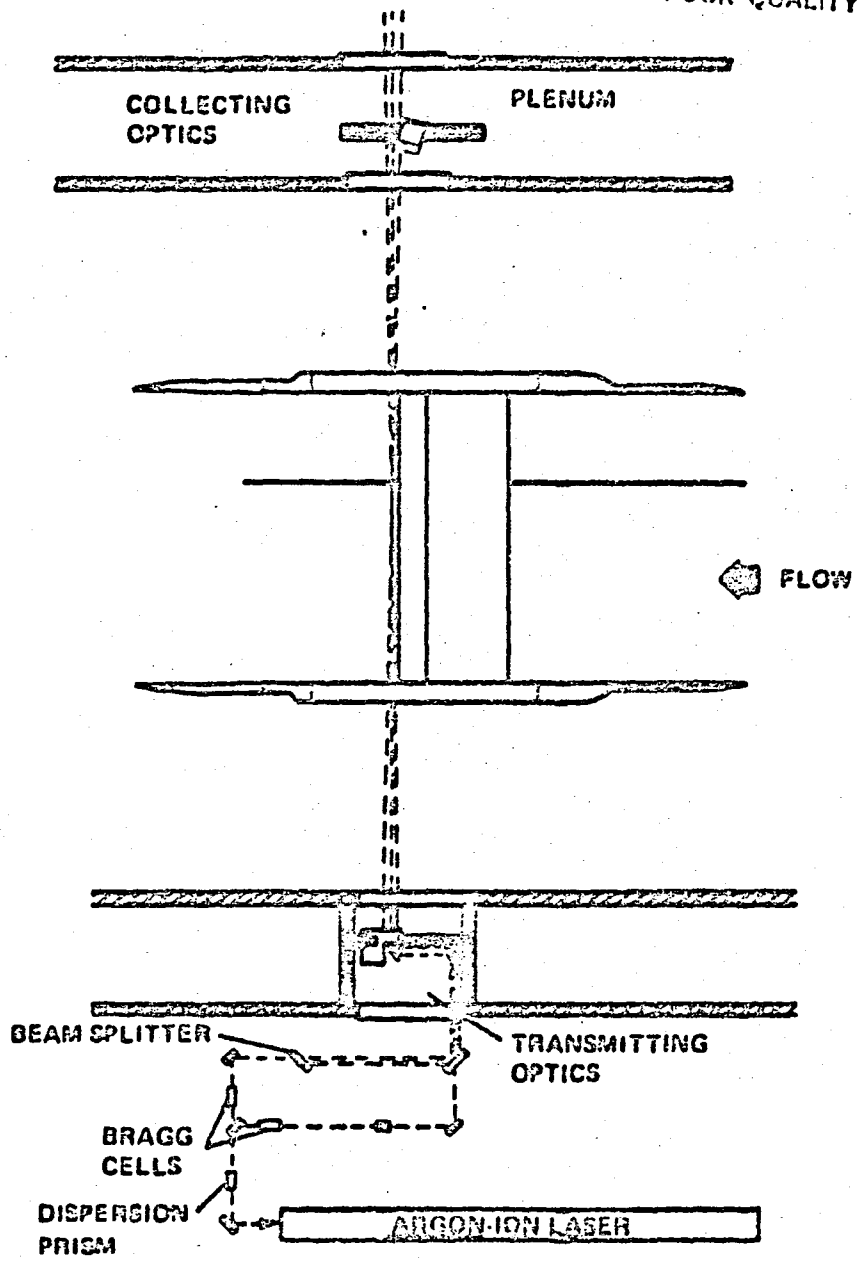

Fig. 1b Laser Velocimeter Installation in Ames 11-foot Wind Tunnel.

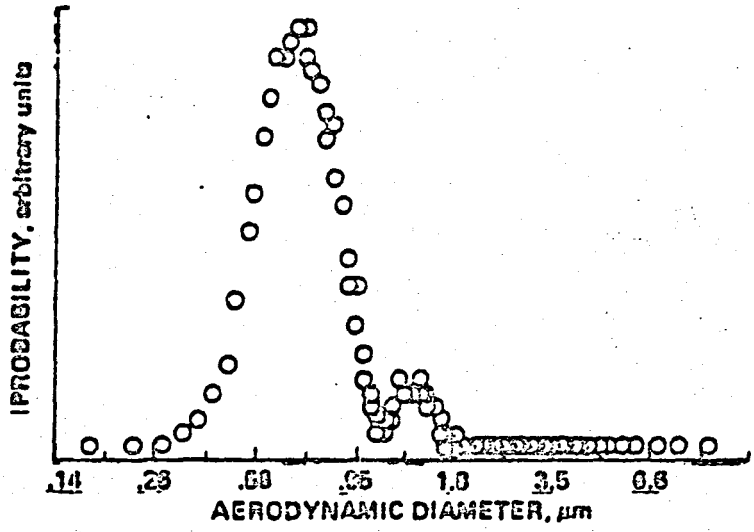

Fig. 2 Seed Particle Size Distribution

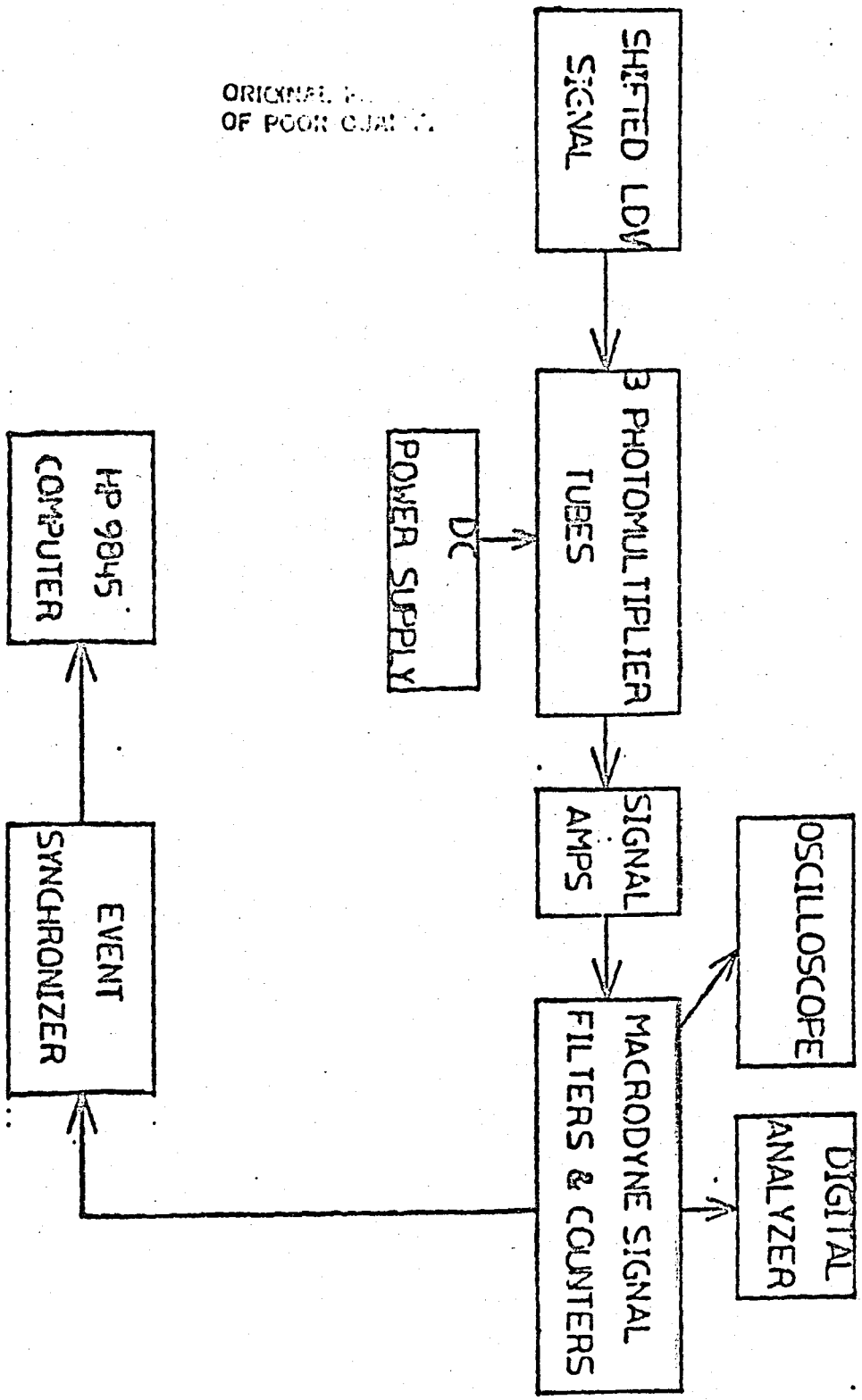

Fig. 3 Signal Processing Electronics

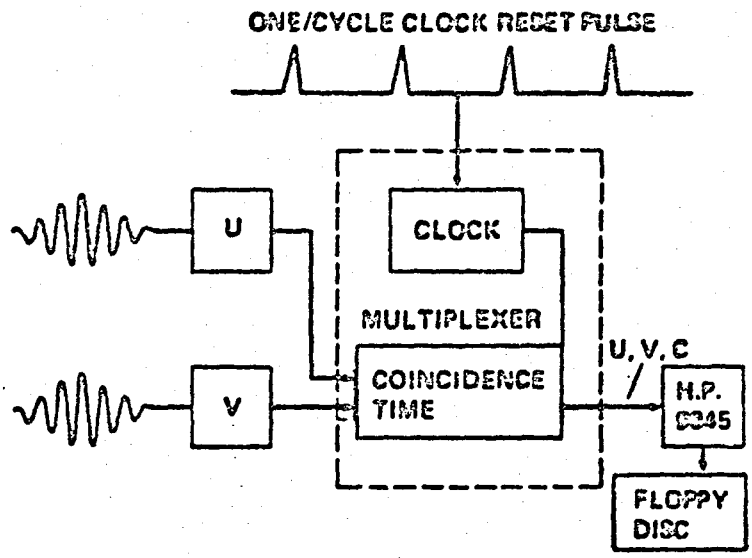

Fig. 4 Conditional Sampling Data System

X = -2.540 cm Alpha = +0.0° Freq = 0.00 Hz
Z = 0.000 cm Delta = +0.0° Uinf (LDV)= 261.3 m/s
Mach= 0.000 Mean Delta=+0.0° Uedge (LDV)= 264.2 m/s
Reyn=6500000 Amplitude =±0.0° Uedge (HW) = 260.9 m/s

LDV DATA (STATIC)

Y cm	U/Ue	V/Ue	U1/Ue	V1/Ue
1.524	0.9947	-0.0236	0.0257	0.0403
1.270	0.9861	-0.0245	0.0298	0.0393
1.143	0.9810	-0.0232	0.0312	0.0444
1.016	0.9749	-0.0226	0.0383	0.0406
0.889	0.9649	-0.0220	0.0416	0.0505
0.762	0.9434	-0.0238	0.0483	0.0468
0.635	0.9119	-0.0141	0.0950	0.0860
0.508	0.8796	-0.0276	0.1002	0.0979
0.381	0.8417	-0.0240	0.0939	0.1086
0.254	0.7862	-0.0193	0.1016	0.1061
0.127	0.7492	-0.0296	0.1061	0.1347
0.000	0.6929	-0.0218	0.0895	0.1234
-0.127	0.7126	0.0079	0.0870	0.0764
-0.254	0.8003	0.0176	0.0624	0.0645
-0.381	0.8575	0.0243	0.0770	0.0639
-0.508	0.9083	0.0239	0.0602	0.0603
-0.635	0.9571	0.0229	0.0431	0.0601
-0.762	0.9700	0.0242	0.0314	0.0545
-0.889	0.9885	0.0204	0.0257	0.0439
-1.016	0.9943	0.0108	0.0233	0.0464
-1.143	0.9951	0.0208	0.0222	0.0416
-1.270	0.9967	0.0157	0.0249	0.0438
-1.397	1.0000	0.0203	0.0211	0.0443

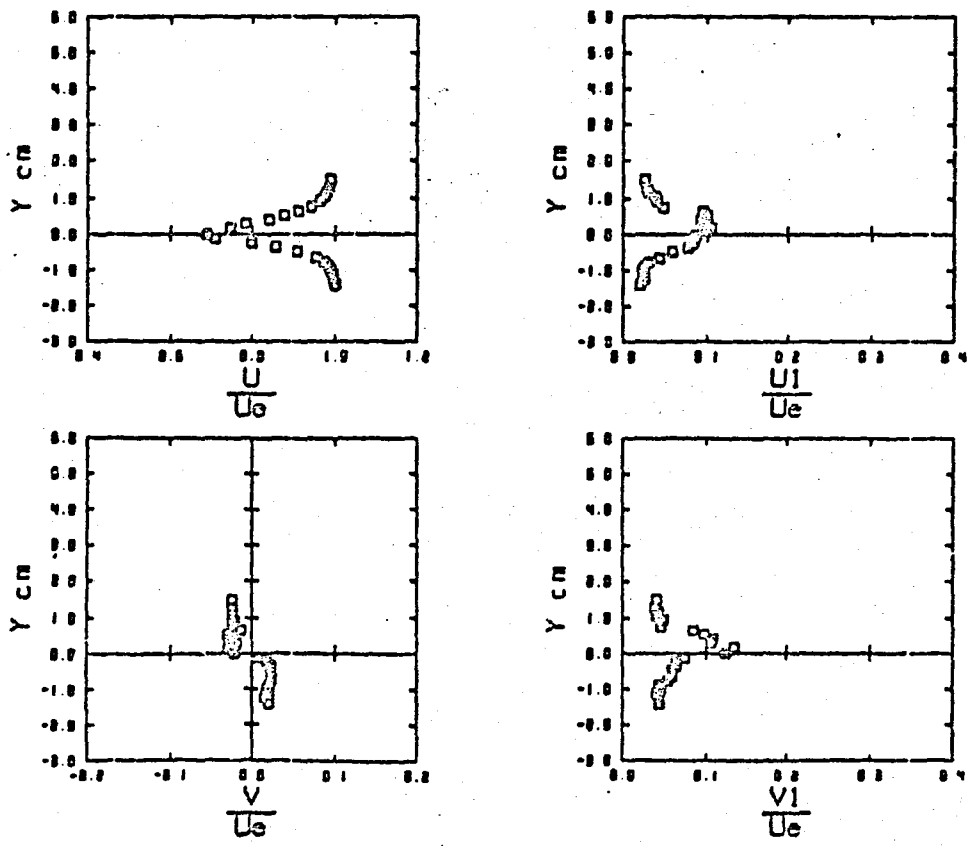

Fig. 5 Laser Velocimeter Data

X	=-12.700 cm	Alpha	=+0.0°	Freq	= 0.00 Hz
Z	= 0.000 cm	Delta	=+0.0°	Uinf (LDV)=	261.3 m/s
Mach=	0.600	Mean Delta	=+0.0°	Uedge (LDV)=	264.2 m/s
Reyn=	6500000	Amplitude	=±0.0°	Uedge (HW) =	264.5 m/s

LDV DATA (STATIC)

Y cm	U/Ue	V/Ue	U1/Ue	V1/Ue
2.413	0.9935	-0.0063	0.0237	0.0311
2.159	1.0000	-0.0052	0.0260	0.0317
1.905	0.9997	-0.0235	0.0224	0.0321
1.651	0.9981	-0.0043	0.0272	0.0355
1.397	0.9944	-0.0043	0.0204	0.0303
1.143	0.9885	-0.0125	0.0318	0.0434
0.889	0.9524	-0.0126	0.0403	0.0479
0.635	0.0924	-0.0082	0.0701	0.0652
0.381	0.0244	-0.0044	0.0561	0.0506
0.127	0.0001	0.0001	0.0407	0.0556
-0.127	0.0042	0.0009	0.0520	0.0449
-0.381	0.0350	0.0023	0.0699	0.0428
-0.635	0.9018	0.0020	0.0867	0.0376
-0.889	0.9826	0.0061	0.0343	0.0290
-1.143	0.9967	0.0041	0.0311	0.0324

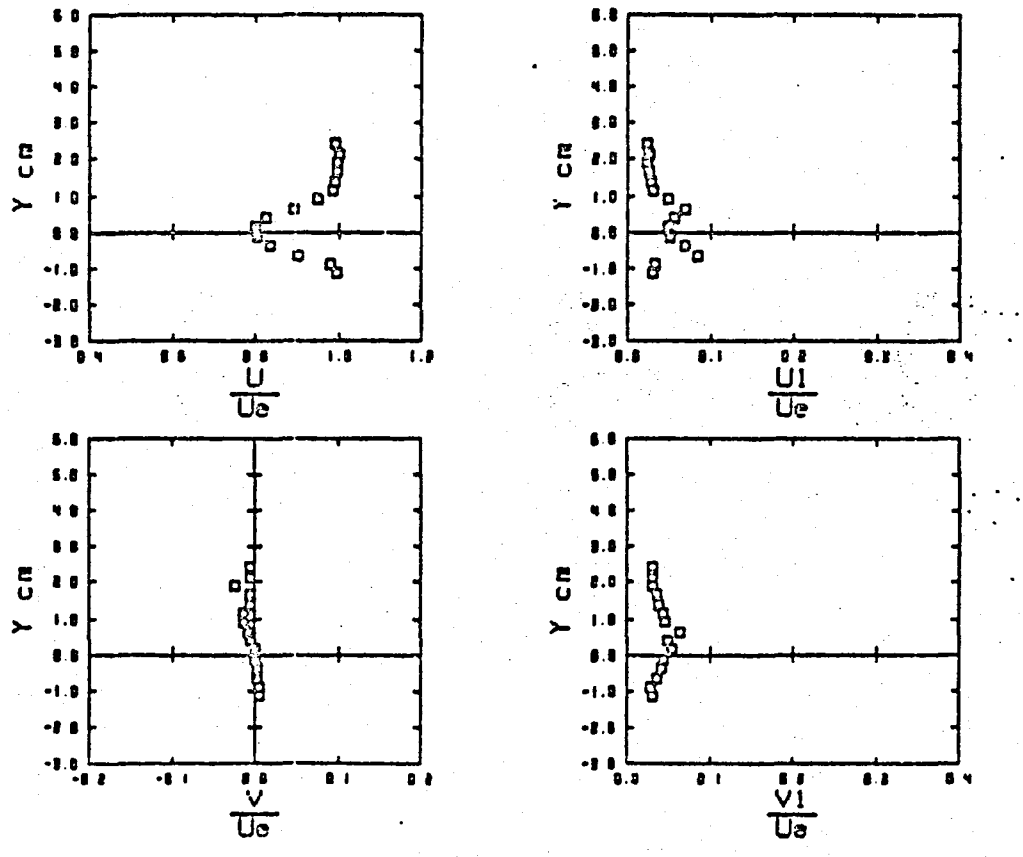

Fig. 6 Laser Velocimeter Data

X = -2.540 cm Alpha = +0.0° Freq = 0.00 Hz
Z = 0.000 cm Delta = -4.0° Uinf (LDV)= 261.3 m/s
Mach= 0.000 Mean Delta=-4.0° Uedge (LDV)= 264.2 m/s
Reyn=6500000 Amplitude =±0.0° Uedge (HW) = 256.0 m/s

LDV DATA (STATIC)

Y cm	U/Ue	V/Ue	U1/Ue	V1/Ue
2.032	0.9991	0.0039	0.0219	0.0476
1.778	0.9963	0.0034	0.0268	0.0451
1.651	0.9916	0.0076	0.0270	0.0472
1.524	0.9801	0.0112	0.0324	0.0462
1.397	0.9461	0.0031	0.0486	0.0499
1.270	0.8866	0.0070	0.0687	0.0534
1.143	0.7999	-0.0026	0.0893	0.0593
1.016	0.6987	0.0010	0.0879	0.0757
0.889	0.6384	0.0296	0.0914	0.0956
0.762	0.6584	0.0599	0.1072	0.0976
0.635	0.7120	0.0817	0.1217	0.0961
0.508	0.7965	0.0789	0.1001	0.0931
0.381	0.8618	0.0928	0.0858	0.0774
0.254	0.9002	0.0956	0.0768	0.0639
0.127	0.9503	0.0915	0.0497	0.0609
0.000	0.9670	0.0809	0.0405	0.0587
-0.127	0.9833	0.0846	0.0344	0.0536
-0.254	0.9841	0.0755	0.0285	0.0502
-0.381	1.0000	0.0777	0.0320	0.0478
-0.508	0.9970	0.0772	0.0290	0.0468

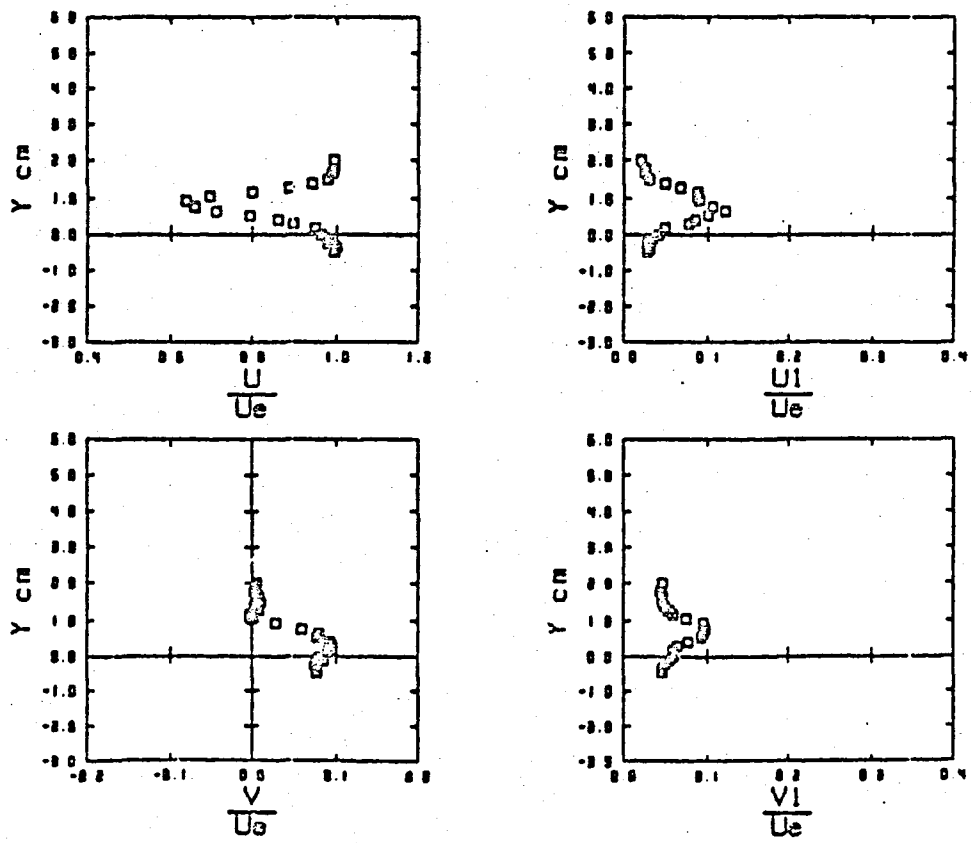

Fig. 7 Laser Velocimeter Data

X = -2.540 cm		Alpha =+4.0°		Freq = 0.00 Hz	
Z = 0.000 cm		Delta =-4.0°		Uinf (LDV)= 261.3 m/s	
Mach= 0.800		Mean Delta=-4.0°		Uedge (LDV)= 264.2 m/s	
Reyn=6500000		Amplitude =±0.0°		Uedge (HW) = 240.1 m/s	

LDV DATA (STATIC)

Y cm	U/Ue	V/Ue	U1/Ue	V1/Ue
4.064	1.0000	-0.1026	0.0338	0.4919
3.556	0.9893	-0.0522	0.0315	0.0481
3.048	0.9719	-0.0548	0.0450	0.0541
2.540	0.9336	-0.0564	0.0494	0.0642
2.286	0.8879	-0.0593	0.0953	0.0712
2.032	0.8312	-0.0493	0.0759	0.0844
1.778	0.8005	-0.0444	0.1169	0.0955
1.524	0.7710	-0.0459	0.1105	0.0940
1.270	0.7176	-0.0419	0.1211	0.0883
1.143	0.6776	-0.0280	0.1184	0.0835
1.016	0.6384	-0.0236	0.1284	0.0906
0.889	0.6351	-0.0105	0.1135	0.0880
0.762	0.6540	-0.0132	0.0951	0.0728
0.635	0.6706	0.0122	0.0999	0.0902
0.508	0.7457	0.0261	0.1101	0.0828
0.381	0.8757	0.0274	0.0589	0.0722
0.254	0.8729	0.0289	0.0956	0.0649
0.127	0.9327	0.0291	0.0625	0.0608
0.000	0.9441	0.0208	0.0551	0.0545
-0.127	0.9745	0.0171	0.0360	0.0465
-0.254	0.9882	0.0165	0.0342	0.0440
-0.381	0.9922	0.0183	0.0294	0.0408
-0.508	0.9943	0.0221	0.0246	0.0439

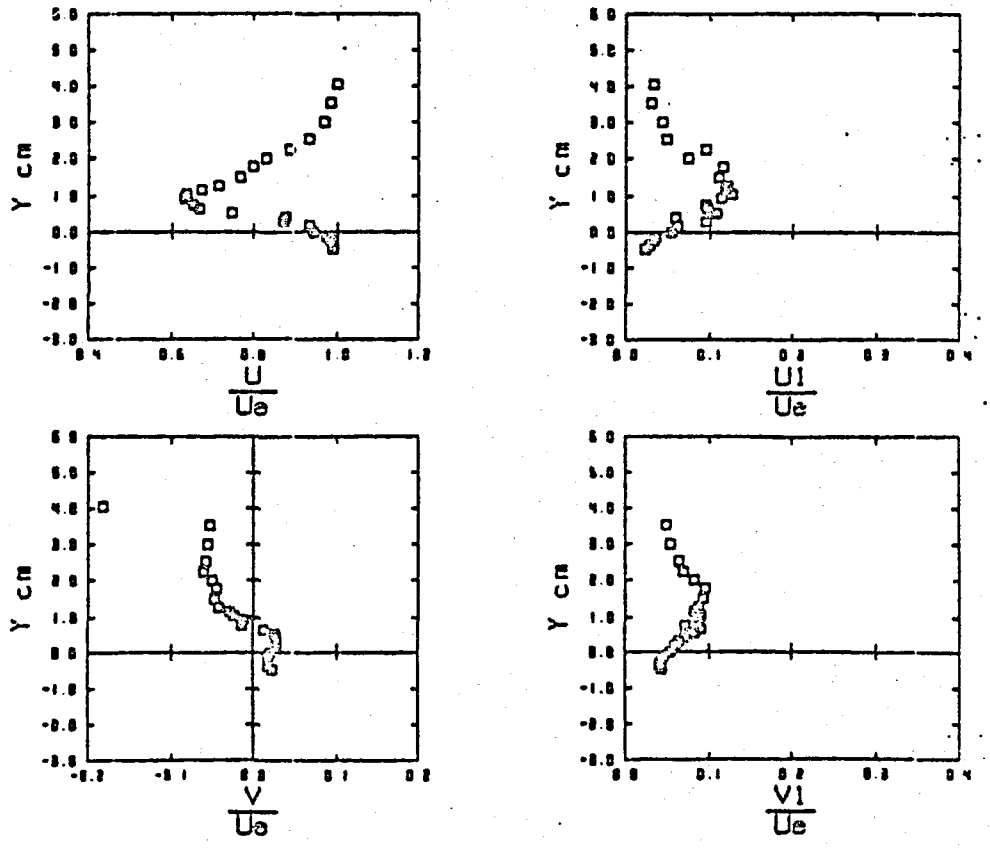

Fig. 8 Laser Velocimeter Data

X =-12.700 cm Alpha =+4.3° Freq = 0.00 Hz
Z = 0.000 cm Delta =-4.0° Uinf (LDV)= 261.3 m/s
Mach= 0.800 Mean Delta=-4.0° Uedge (LDV)= 264.2 m/s
Reyn=6500000 Amplitude =±0.0° Uedge (HW) = 257.3 m/s

LDV DATA (STATIC)

Y cm	U/Ue	V/Ue	U1/Ue	V1/Ue
2.413	0.9917	-0.0741	0.0297	0.0806
1.905	0.9070	-0.0389	0.0347	0.1207
1.651	0.9791	-0.0352	0.0469	0.1199
1.397	0.9800	-0.0360	0.0387	0.1200
1.143	0.9673	-0.0264	0.0475	0.1238
0.889	0.9058	-0.0225	0.0927	0.1217
0.635	0.8874	-0.0323	0.0940	0.1221
0.381	0.8611	-0.0872	0.0965	0.1179
0.127	0.8207	-0.0144	0.0982	0.1094
-0.127	0.7973	-0.0067	0.0787	0.1113
-0.381	0.7885	-0.0100	0.0751	0.1074
-0.635	0.7936	0.0027	0.0675	0.0929
-0.889	0.8064	-0.0093	0.0705	0.0794
-1.143	0.8379	-0.0105	0.0758	0.0729
-1.397	0.8745	-0.0164	0.0856	0.0681
-1.651	0.9244	-0.0208	0.0915	0.0641
-1.905	1.0000	-0.0190	0.0370	0.0493

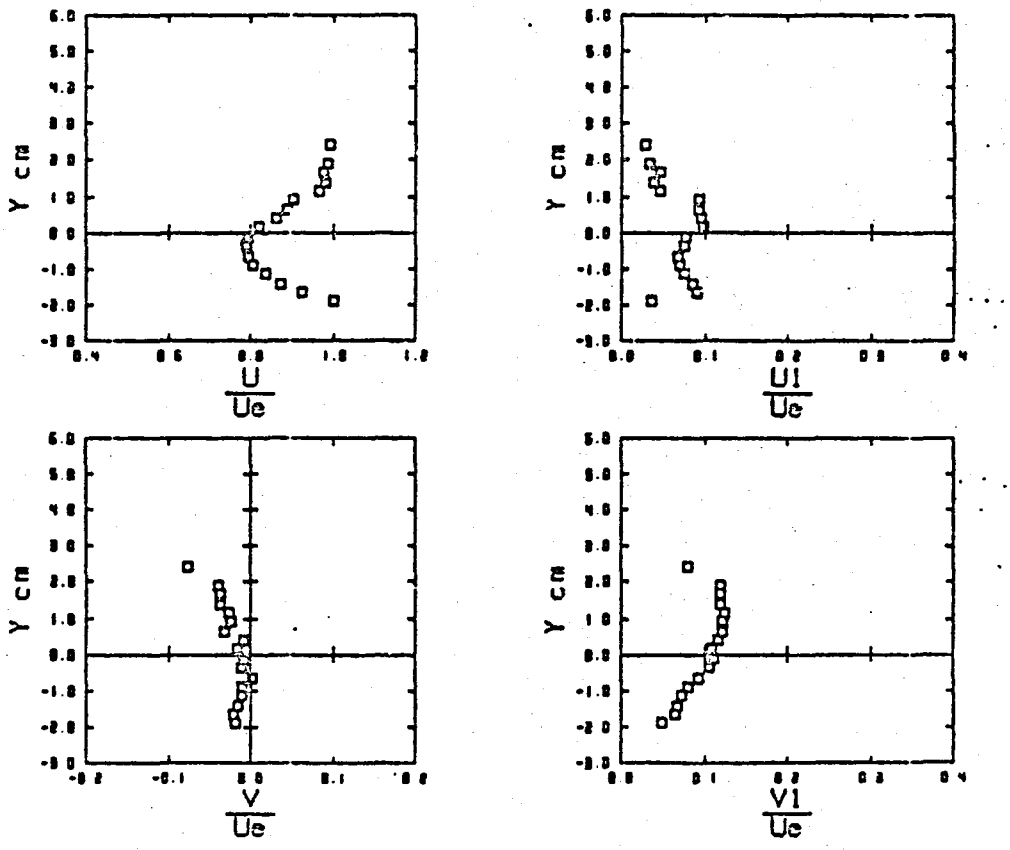

Fig. 9 Laser Velocimeter Data

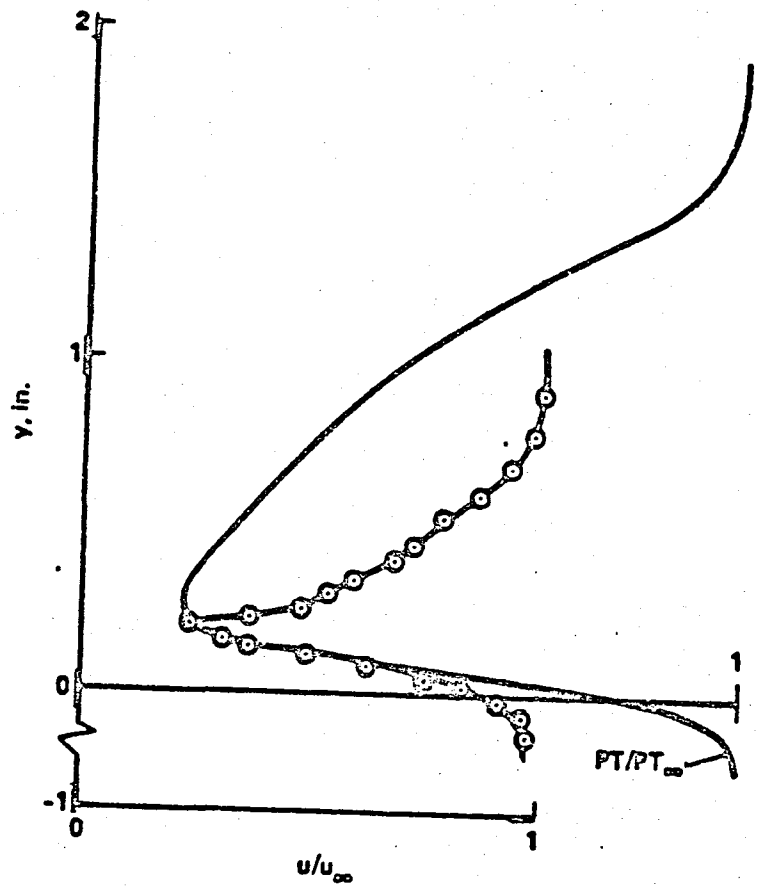

Fig. 10 Comparison of Laser Velocimeter and Pitot Profiles, for a Flap Angle of 4 degrees.

X = -2.540 cm
Z = 0.000 cm
Mach= 0.800
Reyn=6500000

Alpha =+0.0°
Delta =+0.0°
Mean Delta=+0.0°
Amplitude =±0.0°

Freq = 0.00 Hz
Uinf (LDV)= 261.3 m/s
Uedge (LDV)= 264.2 m/s
Uedge (HW) = 260.9 m/s

LDV DATA (STATIC)

Y cm	U/Ue	V/Ue
1.524	0.9947	-0.0236
1.270	0.9861	-0.0245
1.143	0.9810	-0.0232
1.016	0.9749	-0.0226
0.889	0.9649	-0.0220
0.762	0.9434	-0.0238
0.635	0.9119	-0.0141
0.508	0.8796	-0.0276
0.381	0.8417	-0.0248
0.254	0.7862	-0.0193
0.127	0.7492	-0.0296
0.000	0.6929	-0.0218
-.127	0.7126	0.0079
-.254	0.8003	0.0176
-.381	0.8575	0.0243
-.508	0.9083	0.0239
-.635	0.9571	0.0229
-.762	0.9780	0.0242
-.889	0.9885	0.0204
-1.016	0.9943	0.0188
-1.143	0.9951	0.0208
-1.270	0.9967	0.0157
-1.397	1.0000	0.0203

HOT WIRE DATA

Y cm	U/Ue	V/Ue
12.700	1.0000	0.0070
10.160	1.0030	-0.0100
7.620	0.9890	-0.0190
5.080	0.9750	-0.0080
3.810	0.9550	0.0020
2.540	0.9540	-0.0040
1.905	0.9330	0.0140
1.270	0.8940	0.0200
0.635	0.7190	0.0620
0.000	0.6930	0.0440
-.635	0.8910	0.0520
-1.270	0.9240	0.0470
-1.905	0.9190	0.0570
-2.540	0.9360	0.0430
-3.810	0.9370	0.0470
-5.080	0.9380	0.0570
-7.620	0.9660	0.0520

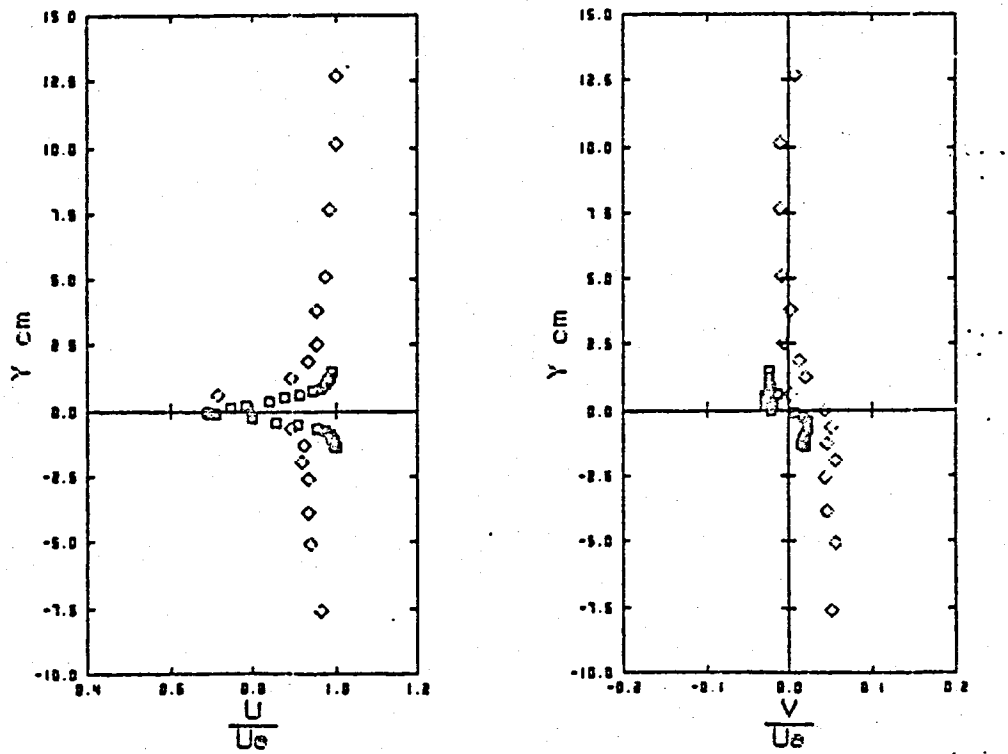

Fig. 11 Comparison of Hot Wire and LDV Measurements

X =-12.700 cm
Z = 0.000 cm
Mach= 0.800
Reyn=6500000

Alpha =+0.0°
Delta =+0.0°
Mean Delta=+0.0°
Amplitude =±0.0°

Freq = 0.00 Hz
Uinf ‹LDV›= 261.3 m/s
Uedge ‹LDV›= 264.2 m/s
Uedge ‹HW› = 264.5 m/s

LDV DATA (STATIC)

Y cm	U/Ue	V/Ue
2.413	0.9935	-0.0063
2.159	1.0000	-0.0052
1.905	0.9997	-0.0235
1.651	0.9981	-0.0043
1.397	0.9944	-0.0043
1.143	0.9885	-0.0125
0.889	0.9524	-0.0126
0.635	0.8924	-0.0092
0.381	0.8244	-0.0044
0.127	0.8001	0.0001
-.127	0.8042	0.0009
-.381	0.8350	0.0023
-.635	0.9018	0.0020
-.889	0.9626	0.0061
-1.143	0.9967	0.0041

HOT WIRE DATA

Y cm	U/Ue	V/Ue
12.700	1.0000	0.0430
10.160	1.0190	0.0250
7.620	1.0070	0.0290
5.080	1.0140	0.0240
3.810	0.9970	0.3770
2.540	1.0110	0.0260
1.905	1.0160	0.0200
1.270	0.9820	0.0160
0.635	0.8820	0.0260
0.000	0.8600	0.0320
-.635	0.9420	0.0340
-1.270	0.9780	0.0390
-1.905	0.9980	0.0460
-2.540	0.9920	0.0400
-3.810	0.9920	0.0540
-5.080	1.0050	0.0400
-7.620	1.0230	0.0330

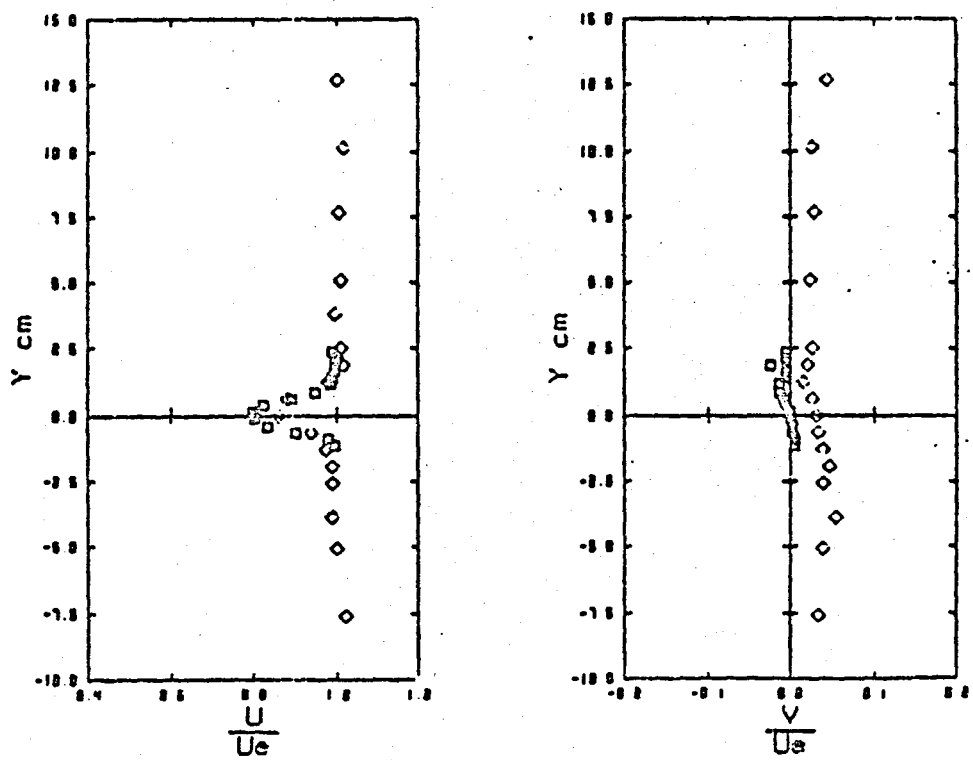

Fig. 12 Comparison of Hot Wire and LDV Measurements

X = -2.540 cm
Z = 0.000 cm
Mach= 0.800
Reyn=6500000

Alpha =+0.0°
Delta =-4.0°
Mean Delta=-4.0°
Amplitude =±0.0°

Freq = 0.00 Hz
Uinf (LDV)= 261.3 m/s
Uedge (LDV)= 264.2 m/s
Uedge (HW) = 256.0 m/s

LDV DATA (STATIC)

Y cm	U/Ue	V/Ue
2.032	0.9991	0.0039
1.778	0.9963	0.0034
1.651	0.9916	0.0076
1.524	0.9801	0.0112
1.397	0.9461	0.0031
1.270	0.8866	0.0070
1.143	0.7999	-0.0026
1.016	0.6987	0.0010
0.889	0.6384	0.0296
0.762	0.6584	0.0599
0.635	0.7120	0.0817
0.508	0.7965	0.0789
0.381	0.8618	0.0928
0.254	0.9002	0.0956
0.127	0.9503	0.0915
0.000	0.9670	0.0869
-.127	0.9833	0.0846
-.254	0.9841	0.0755
-.381	1.0000	0.0777
-.508	0.9970	0.0772

HOT WIRE DATA

Y cm	U/Ue	V/Ue
12.700	1.0000	0.0220
7.620	0.9870	0.0210
3.810	0.9480	0.0330
2.540	0.9520	0.0080
1.905	0.9610	0.0210
1.524	0.8420	-0.0130
1.270	0.6000	-0.0030
0.635	0.5390	0.0540
0.330	0.6260	0.0820
0.000	0.6750	0.1020
-.635	0.8840	0.1070
-1.905	0.9250	0.1050
-3.810	0.9490	0.0980
-7.620	0.9700	0.1160

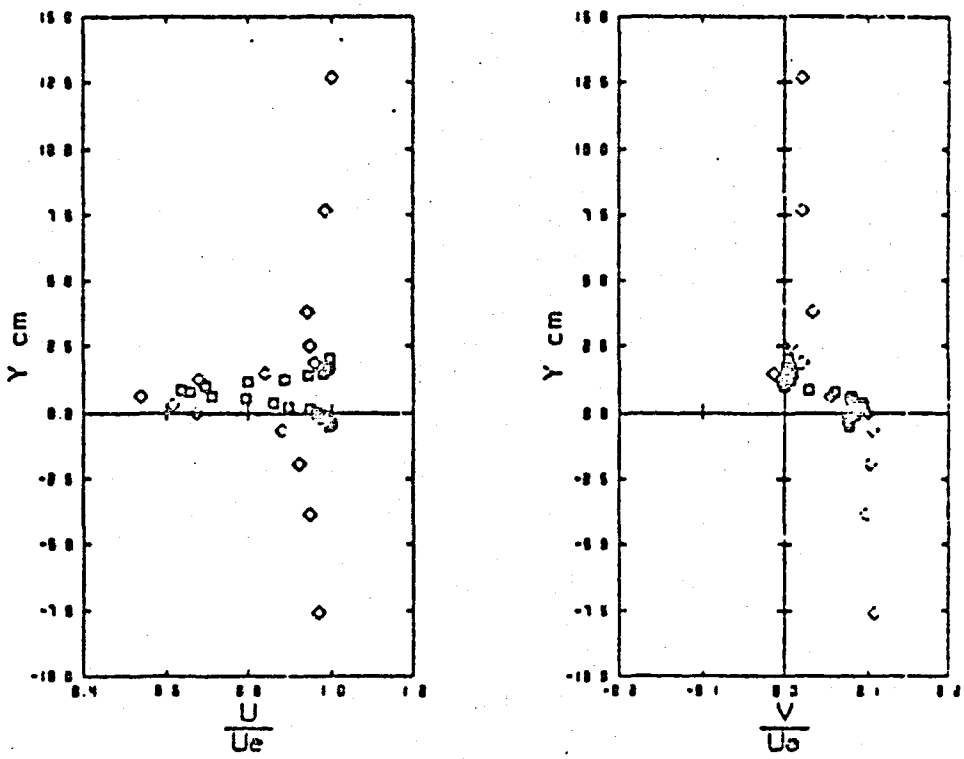

Fig. 13 Comparison of Hot Wire and LDV Measurements

X = -2.540 cm
Z = 0.000 cm
Mach= 0.800
Reyn=6500000

Alpha = +4.0°
Delta = -4.0°
Mean Delta=-4.0°
Amplitude =20.0°

Freq = 0.00 Hz
Uinf (LDV)= 261.3 m/s
Uedge (LDV)= 264.2 m/s
Uedge (HW) = 240.1 m/s

LDV DATA (STATIC)

Y cm	U/Ue	V/Ue
4.064	1.0000	-0.1026
3.556	0.9893	-0.0522
3.048	0.9719	-0.0548
2.540	0.9336	-0.0584
2.286	0.8079	-0.0593
2.032	0.8312	-0.0493
1.778	0.8005	-0.0444
1.524	0.7710	-0.0459
1.270	0.7176	-0.0419
1.143	0.6776	-0.0280
1.016	0.6384	-0.0236
0.889	0.6351	-0.0105
0.762	0.6540	-0.0132
0.635	0.6708	0.0122
0.508	0.7457	0.0261
0.381	0.8757	0.0274
0.254	0.8729	0.0289
0.127	0.9327	0.0291
0.000	0.9441	0.0208
-.127	0.9745	0.0171
-.254	0.9882	0.0165
-.381	0.9922	0.0183
-.508	0.9943	0.0221

HOT WIRE DATA

Y cm	U/Ue	V/Ue
7.620	1.0000	-0.0230
5.080	0.7970	0.0100
3.810	0.6910	0.0320
3.175	0.6520	0.0060
2.540	0.6200	0.0420
1.905	0.5910	0.0420
1.600	0.5630	0.0400
1.270	0.5520	0.0510
0.965	0.6000	0.0670
0.635	0.7130	0.0590
0.080	0.9710	0.0590
-.635	0.9600	0.0540
-1.270	0.9970	0.0500
-2.540	1.0150	0.0610
-7.620	1.0680	0.0480

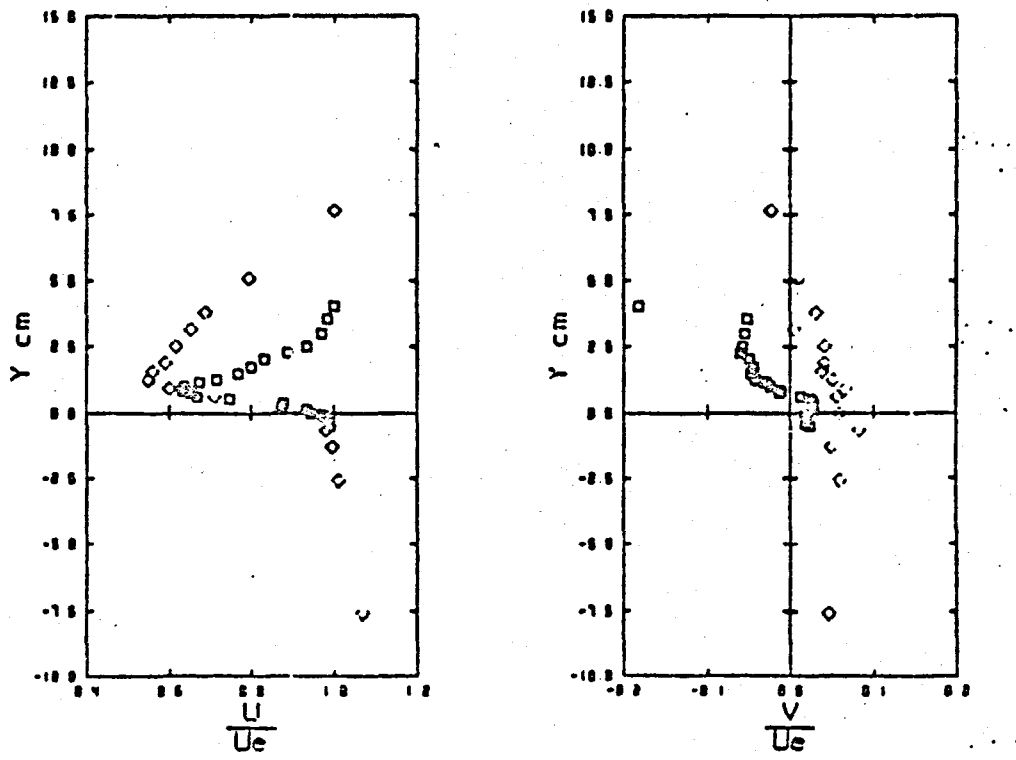

Fig. 14 Comparison of Hot Wire and LDV Measurements

X = -12.700 cm	Alpha = +4.6°	Freq = 0.00 Hz
Z = 0.000 cm	Delta = -4.0°	Uinf (LDV) = 261.3 m/s
Mach = 0.000	Mean Delta = -4.0°	Uedge (LDV) = 264.2 m/s
Reyn = 6500000	Amplitude = ±0.6°	Uedge (HW) = 257.3 m/s

LDV DATA (STATIC)

Y cm	U/Ue	V/Ue
2.413	0.9917	-0.0741
1.905	0.9870	-0.0389
1.651	0.9791	-0.0352
1.397	0.9800	-0.0360
1.143	0.9673	-0.0264
0.869	0.9056	-0.0225
0.635	0.8074	-0.0323
0.301	0.8611	-0.0072
0.127	0.8207	-0.0144
-.127	0.7973	-0.0067
-.381	0.7885	-0.0100
-.635	0.7936	0.0027
-.889	0.8064	-0.0093
-1.143	0.8379	-0.0105
-1.397	0.8745	-0.0164
-1.651	0.9244	-0.0208
-1.905	1.0000	-0.0190

HOT WIRE DATA

Y cm	U/Ue	V/Ue
7.620	1.0000	0.0020
5.080	0.9130	0.0360
3.810	0.0690	0.0500
3.175	0.0600	0.0400
2.540	0.0540	0.0350
1.905	0.0640	0.0330
1.270	0.0750	0.0210
0.635	0.9080	0.0370
0.000	0.9750	0.0280
-.635	1.0280	0.0180
-1.270	1.0790	0.0120
-2.540	1.0680	0.0310
-7.620	1.0890	0.0300

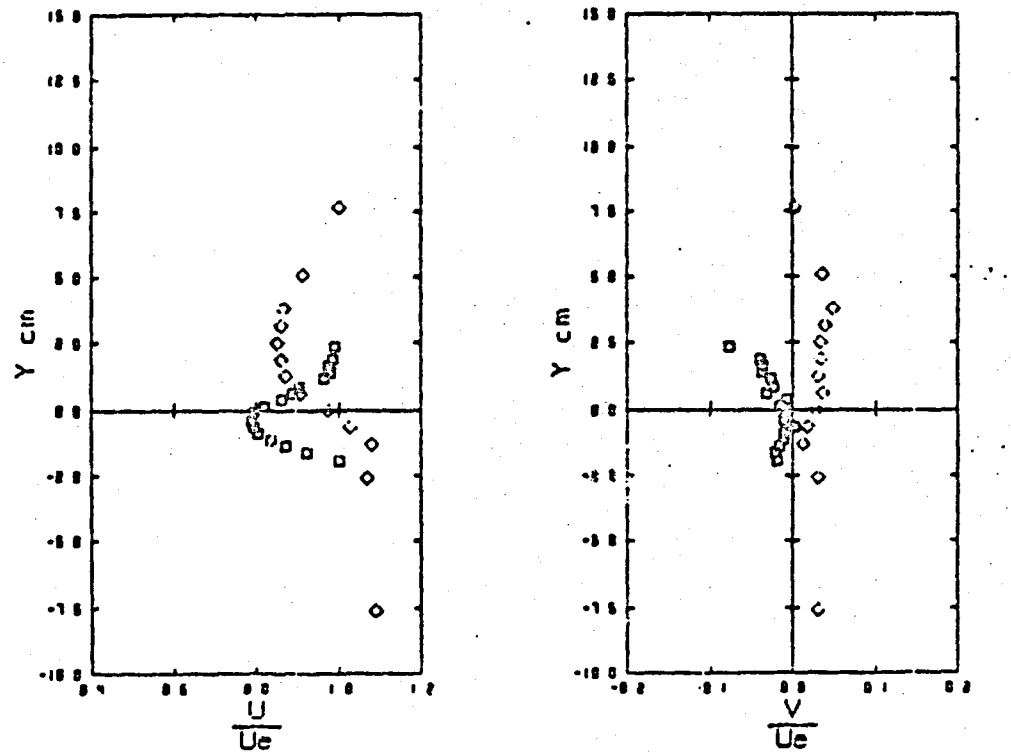

Fig. 15 Comparison of Hot Wire and LDV Measurements

X	= -2.540 cm	Alpha	=+0.0°	Freq	= 30.00 Hz
Z	= 0.000 cm	Delta	=-2.0°	Uinf (LDV)	= 261.3 m/s
Mach= 0.800		Mean Delta	=-4.0°	Uedge (LDV)	= 270.9 m/s
Reyn=6500000		Amplitude	=±2.0°	Uedge (NH)	= 257.6 m/s

LDV DATA (DYNAMIC)

Y cm	U/Ue	V/Ue	U1/Ue	V1/Ue
2.794	1.0000	-0.0081	0.0240	0.0350
2.540	0.9913	-0.0140	0.0250	0.0300
2.286	0.9874	-0.0030	0.0250	0.0630
2.032	0.9814	-0.0017	0.0290	0.0400
1.778	0.9644	-0.0039	0.0330	0.0700
1.524	0.9398	-0.0037	0.0490	0.0800
1.270	0.7526	0.0089	0.0760	0.0500
1.016	0.7061	0.0369	0.0640	0.0620
0.762	0.7203	0.0417	0.0890	0.0850
0.508	0.7897	0.0286	0.0930	0.0630
0.254	0.8471	0.0316	0.0900	0.0480
0.000	0.9202	0.0300	0.0610	0.0460

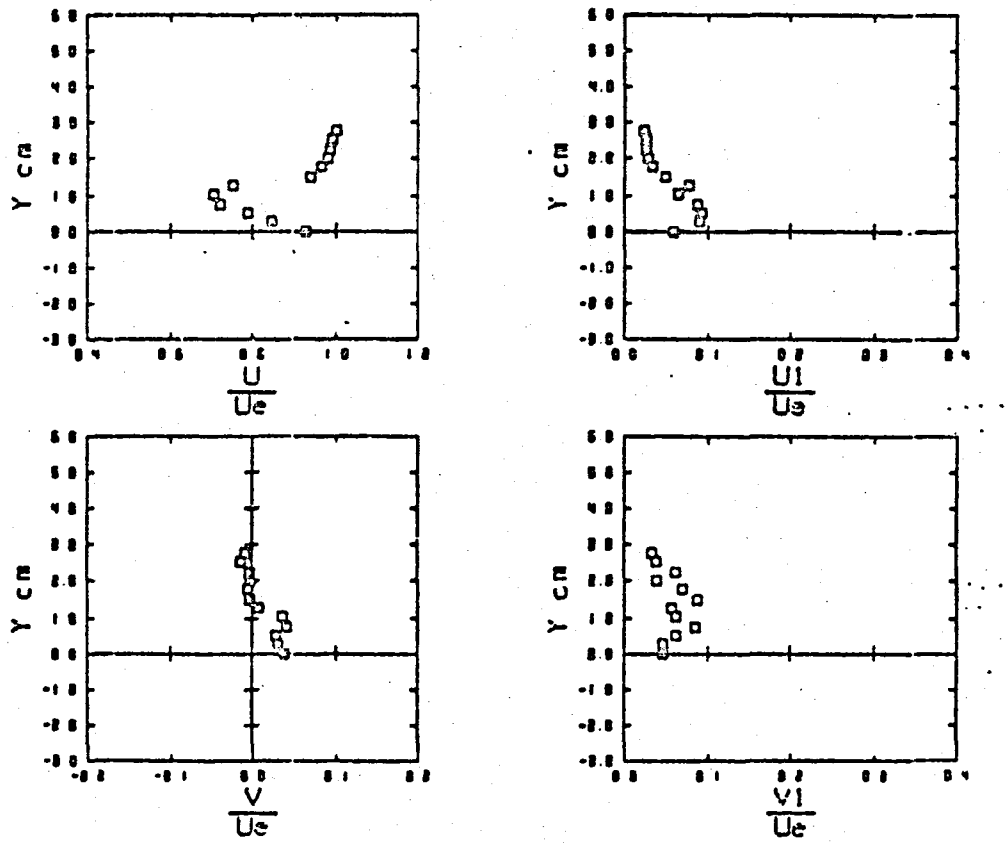

Fig. 16 Comparison of Hot Wire and LDV Measurements

X	= -2.540 cm	Alpha	=+0.0°	Freq	= 30.00 Hz
Z	= 0.000 cm	Delta	=-4.0°	Uinf (LDV)	= 261.3 m/s
Mach=	0.000	Mean Delta	=-4.0°	Uedge (LDV)	= 270.2 m/s
Reyn=	6500000	Amplitude	=±2.0°	Uedge (HW)	= 257.6 m/s

LDV DATA (DYNAMIC)

Y cm	U/Ue	V/Ue	U1/Ue	V1/Ue
2.794	1.0000	-0.0154	0.0220	0.0480
2.540	0.9972	-0.0131	0.0240	0.0350
2.286	0.9913	-0.0124	0.0250	0.0370
2.032	0.9791	-0.0089	0.0240	0.0390
1.778	0.9565	0.0213	0.0400	0.0730
1.524	0.8034	0.0304	0.1110	0.1000
1.270	0.6502	0.0405	0.0920	0.1100
1.016	0.6635	0.0487	0.0900	0.0890
0.762	0.7385	0.0655	0.1290	0.0680
0.508	0.8551	0.0602	0.1220	0.0500
0.254	0.9252	0.0396	0.0820	0.0410
0.000	0.9793	0.0396	0.0400	0.0430

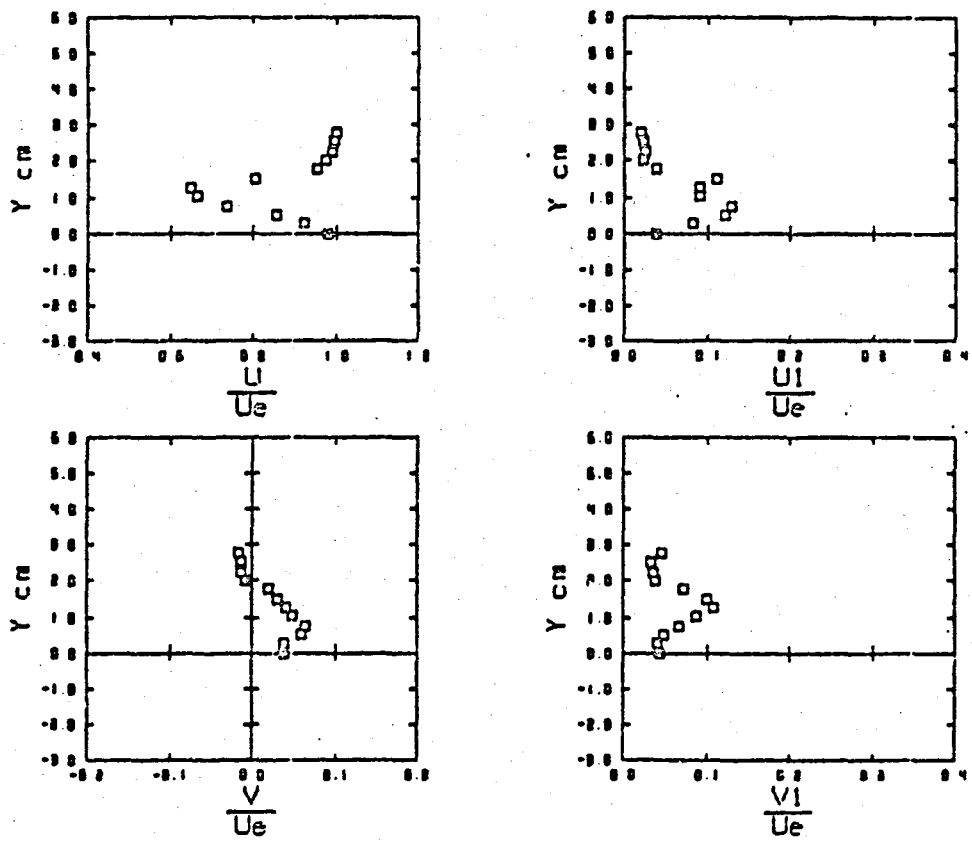

Fig. 17 Comparison of Hot Wire and LDV Measurements

X	= -2.540 cm	Alpha	=+0.0°	Freq	= 30.00 Hz
Z	= 0.000 cm	Delta	=-6.0°	Uinf ⟨LDV⟩	= 261.3 m/s
Mach=	0.800	Mean Delta	=-4.0°	Uedge ⟨LDV⟩	= 272.7 m/s
Re/m=6500000		Amplitude	=±2.0°	Uedge ⟨HW⟩	= 257.6 m/s

LDV DATA (DYNAMIC)

Y cm	U/Ue	V/Ue	U1/Ue	V1/Ue
2.794	1.0000	-0.0004	0.0230	0.0380
2.540	0.9881	-0.0020	0.0220	0.0410
2.286	0.9769	-0.0050	0.0250	0.0510
2.032	0.9591	-0.0013	0.0310	0.0440
1.778	0.6263	0.0143	0.0990	0.1210
1.524	0.6065	0.0486	0.1070	0.1340
1.270	0.5629	0.0904	0.1460	0.0940
1.016	0.6448	0.0838	0.1690	0.0740
0.762	0.8033	0.0807	0.1280	0.0610
0.508	0.8981	0.0739	0.0830	0.0590
0.254	0.9446	0.0739	0.0500	0.0470
0.000	0.9602	0.0710	0.0420	0.0450

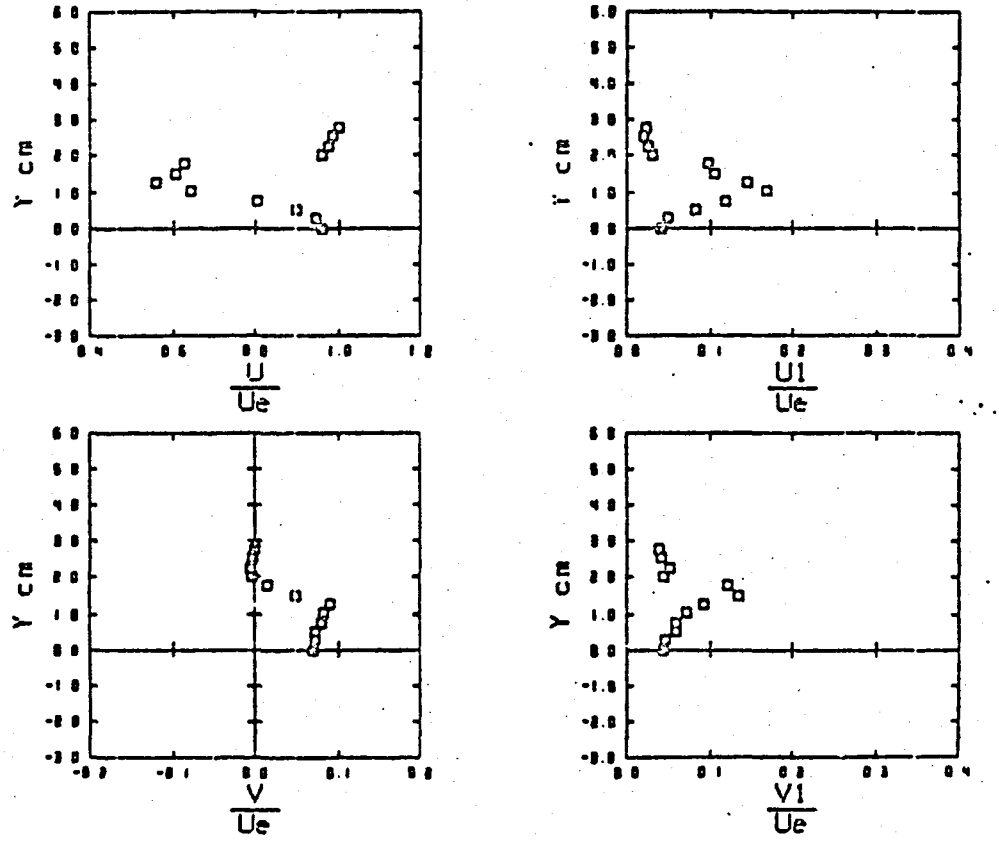

Fig. 18 Comparison of Hot Wire and LDV Measurements

X = -2.540 cm Alpha = -10.0
Z = 0.000 cm Delta = -2.0° Uinf (LDV)= 261.3 m/s
Mach= 0.800 Mean Delta=-4.0° Uedge (LDV)= 270.9 m/s
Reyn=6500000 Amplitude =±2.0° Uedge (HW) = 257.6 m/s

LDV DATA (DYNAMIC)

Y cm	U/Ue	V/Ue
2.794	1.0000	-0.0001
2.540	0.9913	-0.0140
2.286	0.9874	-0.0030
2.032	0.9814	-0.0017
1.778	0.9644	-0.0039
1.524	0.9398	-0.0037
1.270	0.7528	0.0009
1.016	0.7061	0.0369
0.762	0.7203	0.0417
0.508	0.7097	0.0206
0.254	0.0471	0.0316
0.000	0.9202	0.0380

HOT WIRE DATA

Y cm	U/Ue	V/Ue
12.700	1.0070	0.0320
7.620	0.9060	0.0170
3.810	0.9670	0.0340
3.302	0.9620	0.0370
2.540	0.9790	0.0210
2.286	0.9490	0.0390
2.032	0.9490	0.0380
1.270	0.8030	0.0180
1.016	0.7300	0.0220
0.762	0.6400	0.0400
0.000	0.0210	0.0690
-1.270	0.9390	0.0730
-3.302	0.9080	0.0750
-7.620	1.0050	0.0910

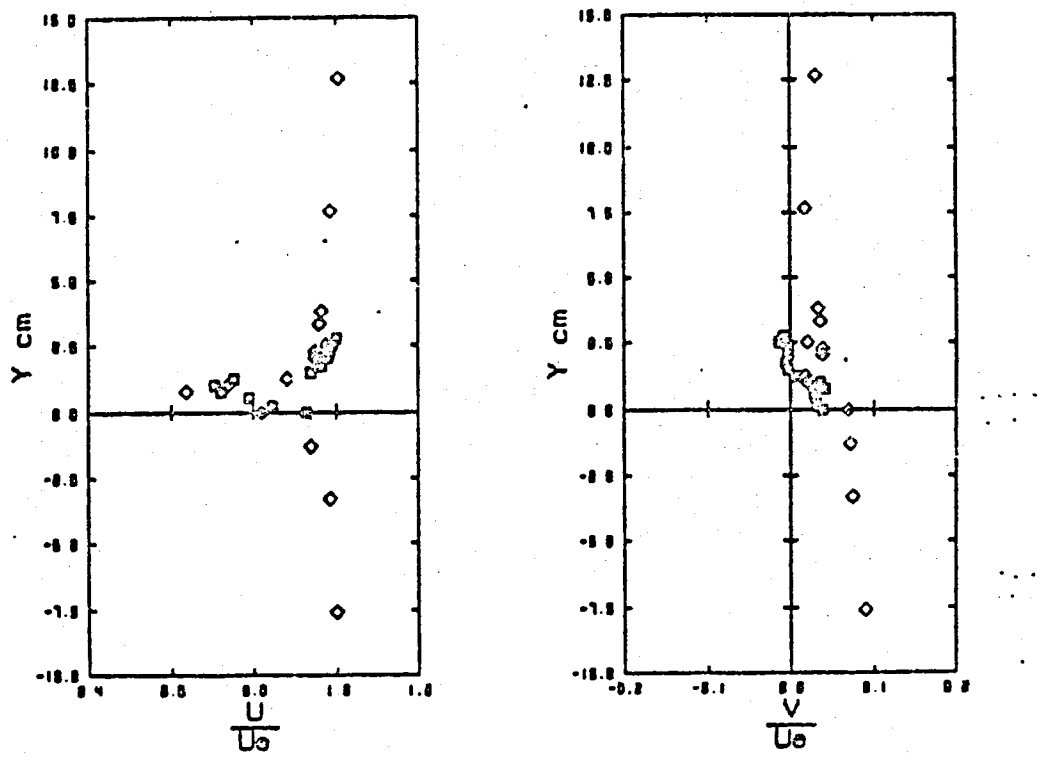

Fig. 19 Comparison of Hot Wire and LDV Measurements

X = -2.540 cm
Z = 0.000 cm
Mach= 0.000
Reyn=6300000

Alpha =+0.0°
Delta =-6.0°
Mean Delta=-4.0°
Amplitude =±2.0°

Freq = 30.00 Hz
Uinf (LDV)= 261.3 m/s
Uedge (LDV)= 272.7 m/s
Uedge (HW) = 257.6 m/s

LDV DATA (DYNAMIC)

Y cm	U/Ue	V/Ue
2.794	1.0000	-0.0004
2.540	0.9881	-0.0020
2.286	0.9769	-0.0050
2.032	0.9591	-0.0013
1.778	0.6263	0.0143
1.524	0.6065	0.0486
1.270	0.5629	0.0904
1.016	0.6448	0.0838
0.762	0.0033	0.0007
0.508	0.0981	0.0739
0.254	0.9446	0.0739
0.000	0.9692	0.0710

HOT WIRE DATA

Y cm	U/Ue	V/Ue
12.700	0.9800	0.0480
7.620	0.9090	0.0230
3.810	0.9010	0.0110
3.302	0.9790	0.0020
2.540	0.9960	-0.0300
2.286	0.9600	-0.0180
2.032	0.9120	-0.0420
1.270	0.6130	-0.0700
1.016	0.4310	-0.0250
0.762	0.4160	0.0350
0.000	0.5070	0.1050
-1.270	0.9050	0.1320
-3.302	1.0250	0.1310
-7.620	1.0610	0.1320

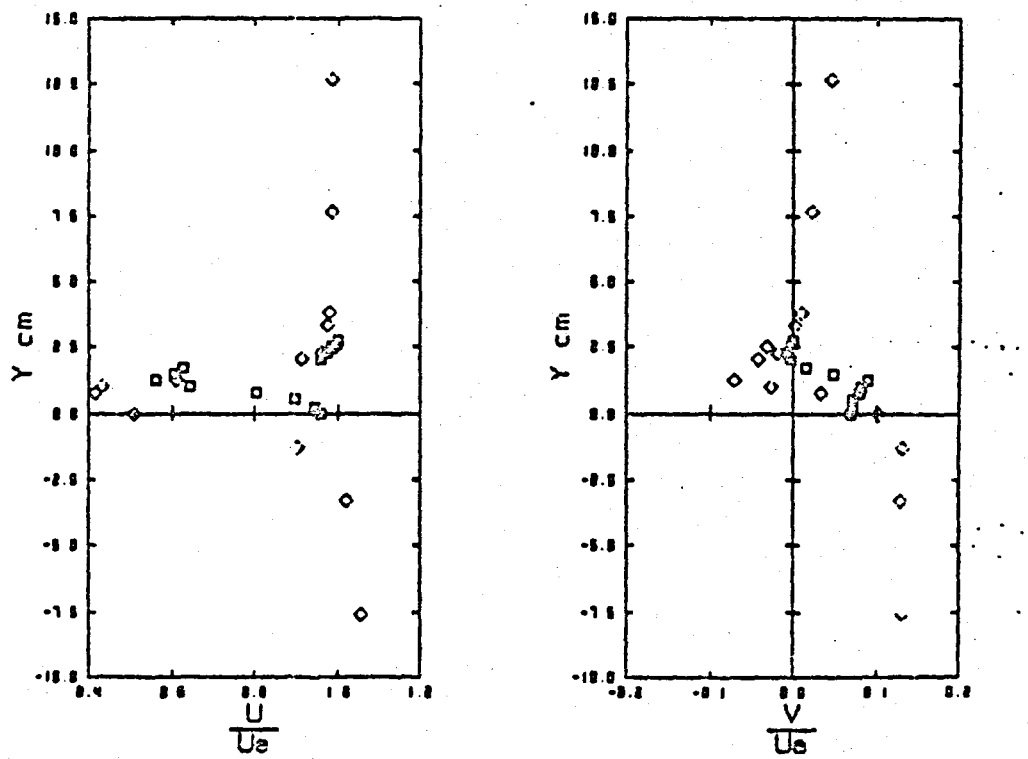

Fig. 20 Comparison of Hot Wire and LDV Measurements

X = -2.540 cm Alpha = +0.0° Freq = 30.00 Hz
Z = 0.000 cm Delta = -4.0° Uinf (LDV)= 261.3 m/s
Mach= 0.800 Mean Delta=-4.0° Uedge (LDV)= 270.2 m/s
Reyn=6500000 Amplitude =±2.0° Uedge (HW) = 257.6 m/s

LDV DATA (DYNAMIC)

Y cm	U/Ue	V/Ue
2.794	1.0000	-0.0154
2.540	0.9972	-0.0131
2.286	0.9913	-0.0124
2.032	0.9791	-0.0089
1.778	0.9565	0.0213
1.524	0.8834	0.0304
1.270	0.6502	0.0405
1.016	0.6635	0.0487
0.762	0.7385	0.0655
0.508	0.8551	0.0602
0.254	0.9252	0.0396
0.000	0.9793	0.0396

HOT WIRE DATA

Y cm	U/Ue	V/Ue
12.700	1.0110	0.0310
7.620	0.9970	0.0090
3.810	0.9820	0.0090
3.302	0.9800	0.0090
2.540	0.9970	-0.0170
2.286	0.9650	-0.0020
2.032	0.9620	-0.0050
1.270	0.8310	-0.0240
1.016	0.5970	-0.0100
0.762	0.4620	-0.0040
0.000	0.4760	0.0610
-1.270	0.8630	0.1210
-3.302	0.9950	0.0970
-7.620	1.0260	0.1020

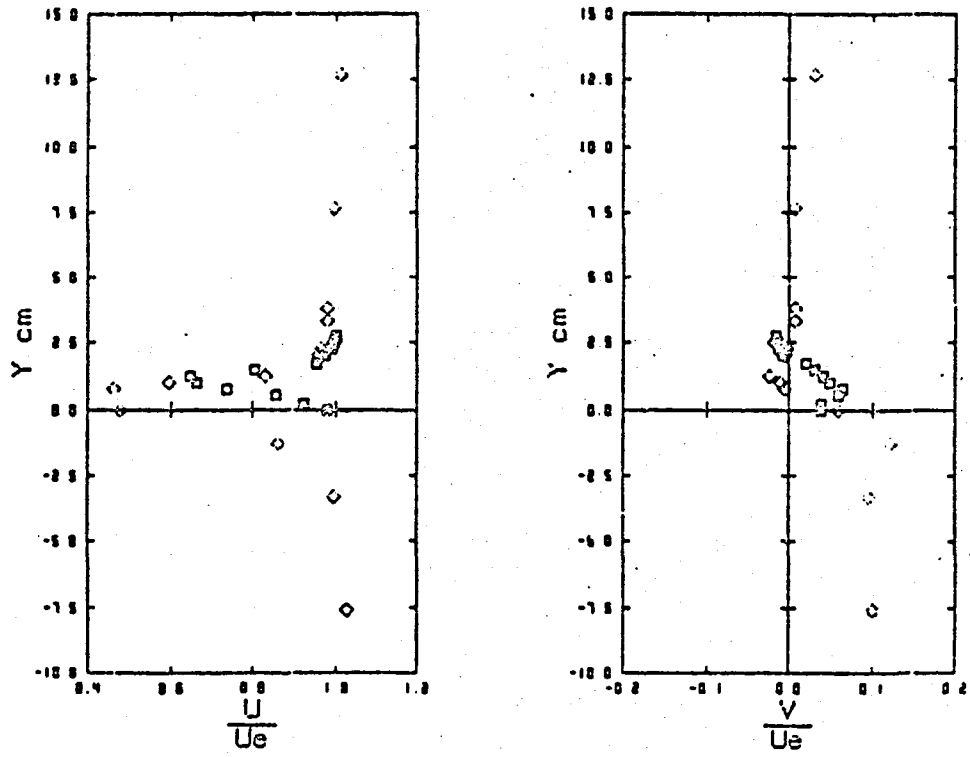

Fig. 21 Comparison of Hot Wire and LDV Measurements

END

DATE

FILMED

DEC 13 1984

End of Document